Journal of Molecular Catalysis B: Enzymatic 113 (2015) 39–46

Contents lists available at ScienceDirect

Journal of Molecular Catalysis B: Enzymatic

journal homepage: www.elsevier.com/locate/molcatb

Structural and functional characterization of a recombinant leucine aminopeptidase

Ana V. Hernández-Moreno[a], Francisco C. Perdomo-Abúndez[a], Victor Pérez-Medina Martínez[a], Gabriel Luna-Bárcenas[b], Francisco Villaseñor-Ortega[c], Néstor O. Pérez[a], Carlos A. López-Morales[a], Luis F. Flores-Ortiz[a], Emilio Medina-Rivero[a,*]

[a] Unidad de Investigación y Desarrollo, PROBIOMED S.A. de C.V., Tenancingo, Estado de México, Mexico
[b] Grupo de investigación de polímeros y biopolímeros, Cinvestav Querétaro, QRO, Mexico
[c] Departamento de Ingeniería Bioquímica, Instituto Tecnológico de Celaya, GTO, Mexico

ARTICLE INFO

Article history:
Received 11 September 2014
Received in revised form
26 December 2014
Accepted 27 December 2014
Available online 3 January 2015

Keywords:
Recombinant leucine aminopeptidase
Folding process
Spectroscopic and thermodynamic techniques
Thermal and chemical stability

ABSTRACT

The function of proteins, such as the catalytic enzyme activity, depends on the interaction of their active sites with their specific substrates and the environment conditions that affect the stability of those sites. This study presents a structure-to-function characterization of the folding process of a recombinant 6×-His tag leucine aminopeptidase (*r*LAP) based on a platform of analytical techniques. The results demonstrated an increase up to 31 U/mg in the activity of the enzyme after folding as revealed by circular dichroism, intrinsic fluorescence, differential scanning calorimetry, and free thiol analysis. Collectively, these techniques revealed a larger number of covalent and non-covalent bonds within the protein seen as an increase in the chemical and thermal stability, while exhibited a lower level of non-bonded cysteines after the protein was folded. Mass spectrometry analysis showed the maintenance of the distribution of the enzyme isoforms related to N-terminal histidine residues after folding, which confirmed that the enzymatic activity of *r*LAP depends on its three-dimensional structure rather than N-terminal self-processing activity. In summary, the studied attributes allow a better understanding of the structure-to-function relationship of *r*LAP, that permit a more proficient manufacturing of the enzyme that would improve the bioprocesses in which is employed.

1. Introduction

DNA technology has been widely used for the production of recombinant proteins such as therapeutic proteins and enzymes. Currently, the production of recombinant proteins in prokaryotic hostess is an advantageous process because allows yielding higher amounts of product [1,2]; nevertheless, the expression of recombinant proteins in *Escherichia coli*, and the purification of insoluble inclusion bodies represent major challenges in determining the correct structure of the recombinant proteins that ensure their biological activity [3–6].

The study of the physical attributes of proteins, and their effects on their biological function, is an important asset in the establishment of the processes and conditions to obtain the appropriate protein structure [7,8]; in addition, is also important to determine the optimal conditions in which these proteins will be preserved and used under specific environments [9–11]. Additionally, identifying the principles of protein folding allows understanding the forces that drive and/or preclude this phenomenon [12,13].

The gaining of knowledge about the relationship between structure, function, and the environment conditions; depends on the study of variables that affect folding, such as: protein concentration, pH, temperature, and ionic strength [14–16]. So, adjustments on the conditions of the protein environment can be planned toward the improvement of its manufacturing bioprocesses. On this regard, enzymes are ideal model proteins, because they act on specific substrates that can be employed to measure their biological activity, and thus investigate the impact of environmental variables on their functionality.

Recombinant leucine aminopeptidase (*r*LAP) is an enzyme commonly used by the biopharmaceutical industry for the remotion of N-terminal methionine [17–21]. The mature 6×-His tag *r*LAP under study is a non-glycosilated monomeric protein of 304 amino acids, with an apparent averaged mass of 32.8 kDa (by reducing SDS-PAGE) [17]. This enzyme exhibits a characteristic secondary structure, as reported by circular dichroism [22]; furthermore, as

* Corresponding author. Tel.: +52 55 11662280; fax: +52 55 53527651.
E-mail address: emilio.medina@probiomed.com.mx (E. Medina-Rivero).

http://dx.doi.org/10.1016/j.molcatb.2014.12.013
1381-1177/

in the wild type leucine aminopeptidase (LAP_{wt}) [19,23], *r*LAP has only one disulfide bond in its mature form which makes easier to study its folding.

In a previous study, we reported an increase in the enzymatic activity of *r*LAP after an incubation period that was conceived as the best for folding [22]. Herein, we focus on the structural changes of *r*LAP and the repercussion on its functional attributes headed to the improvement of bioprocesses.

To achieve this objective, a set of sensitive techniques capable to detect conformational changes in proteins was employed, such as: circular dichroism (CD), intrinsic fluorescence (IF), differential scanning calorimetry (DSC), and mass spectrometry (MS), along with colorimetric free thiol analysis, and enzymatic activity assays that helped to track the changes of *r*LAP subjected to folding and/or induced denaturation. Collectively, these techniques provided a quick and reliable platform to assess structural and functional changes in the protein associated to predetermined variations on its environment.

2. Materials and methods

2.1. Materials

Wild type leucine aminopeptidase from *Vibrio proteolyticus*, Leucine-*p*-nitronilide (L-*p*NA), zinc chloride ($ZnCl_2$), DL-dithiotreitol, tricine, acetonitrile (LC–MS grade), formic acid (LC–MS grade), and water (LC–MS grade) were obtained from Sigma–Aldrich (St. Louis, MO); citric acid, sodium citrate, mono-dibasic sodium phosphate, sodium carbonate, and sodium bicarbonate from J. T. Baker (Center Valley, PA); Urea from Millipore Corp. (Billerica, MA); DyLight 488 Maleimide and Slyde-A-Lyzer 10 kDa MWCO Cassettes from Thermo Fisher Scientific Inc. (Waltham, MA); and Recombinant leucine aminopeptidase (rLAP) in-house produced.

2.2. Activity assay

Enzymatic activity was determined by hydrolysis of L-*p*NA. The assays were conducted by triplicate for each sample of *r*LAP in a final volume of 480 μL; 0.5 mM L-*p*NA and 3×10^{-8} M of purified enzyme were incubated in 10 mM tricine, 1 mM $ZnCl_2$ buffer at pH 8.0. A negative control without enzyme was used to account for non-enzymatic hydrolysis of the substrate. The reactions were incubated at 25 °C for 5 min, and then 20 μL of 20 mM DL-dithiotreitol were added to quench the reaction. Absorbance from *p*-nitroaniline at 405 nm (ε = 10,800 M^{-1} cm^{-1}) [24], and from *r*LAP (ε = 38,700 M^{-1} cm^{-1}) was measured in a Beckman Coulter DU 640 spectrophotometer (Beckman Coulter Inc.; Brea, CA). One enzyme unit (U) was defined as the amount of enzyme that released 1 μmol of *p*-nitroaniline at 25 °C in 1 min.

2.3. Folding conditions

3 μM *r*LAP (in the folding state in which was purified from the inclusion bodies, referred as unfolded) was incubated at 37 °C in 10 mM phosphate, 10 μM $ZnCl_2$ buffer at pH 6.0 for 72 h (main folding conditions). The samples were collected every 12 h to track the enzyme activity. Three different combinations of *r*LAP and $ZnCl_2$ concentrations were also evaluated to observe their effect on the folding process: (1) 30 μM and 20 μM, (2) 152 μM and 50 μM, and (3) 305 μM and 100 μM respectively. After 72 h of folding, the protein was dialyzed in Slyde-A-Lyzer 10 kDa MWCO cassettes, in 10 mM tricine, 1 mM $ZnCl_2$ buffer pH 8.0, at 4 °C, for 24 h; the protein obtained from this step was referred as $rLAP_{fd}$ (folded *r*LAP). Enzyme no subjected to folding was dialyzed under the same conditions prior to be analyzed and was referred as $rLAP_{uf}$ (unfolded *r*LAP). For the mass spectroscopy analysis the enzyme was incubated at 15 °C under the main folding conditions, and was analyzed every 24 h.

2.4. Circular dichroism (CD)

The analysis was conducted at 15 μM of enzyme in the far UV CD region (190–270 nm) at 25 °C using a 0.1 cm path length cell in a Jasco J-815 spectropolarimeter (Jasco Corporation Ltd.; Tokyo, Japan). Three scans per test were accumulated at 1 nm bandwidth.

2.5. Intrinsic fluorescence (IF)

The analysis was conducted at 3 μM of enzyme in 3 mm quartz cells. Fluorescence spectrum was monitored from 290 to 400 nm at 25 °C, using an excitation wavelength of 283 nm in a Fluorolog-3 spectrofluorometer (Horiba Ltd.; Tokyo, Japan). The wavelength of maximal emission (λ_{max}) was defined as the point of maximal intensity from the fluorescence spectra.

2.6. Thermal analysis by IF

IF was monitored in a range from 5 to 90 °C, at a scanning rate of 1 °C min^{-1} using the same instrument and settings mentioned above.

2.7. Fluorescence lifetime using time correlated single photon counting (TCSPC)

Fluorescence lifetime analysis by the Time-Correlated Single Photon Counting method (TCSPC) was performed at 25 °C using 332 nm as emission wavelength, 2 nm band-pass, and a 280 nm ± 10 Nanoled as excitation source. Data analysis was carried out with the DAS6 software (Horiba Ltd.; Tokyo, Japan) using two exponential decay components. The intensity decays were calculated as the sum of exponentials using the Eq. (1) [25].

$$I(t) = \sum_i \alpha_i \exp\left(\frac{-t}{\tau_i}\right) \quad (1)$$

where $\Sigma\alpha_i$ is normalized to the unit, α_i is the pre-exponential factor, and τ_i is the lifetime. The lifetime average (τ) was calculated using the Eq. (2) [26].

$$\langle\tau\rangle = \frac{\sum_{i=1}\alpha_i\tau_i^2}{\sum_{i=1}\alpha_i\tau_i} \quad (2)$$

2.8. Chemical denaturation observed by IF and TCSPC

Solutions of 6 μM *r*LAP were prepared at different concentrations of urea (0–8 M) in 10 mM tricine, 1 mM $ZnCl_2$ buffer at pH 8.0. Urea-induced unfolding was analyzed by IF and TCSPC at 25 °C as described in the methodology of those techniques.

2.9. Chemical denaturation evaluated by enzymatic activity

The urea-induced unfolding of 6 μM *r*LAP was measured by its specific enzymatic activity at different urea concentrations (from 0 to 8 M) in 10 mM tricine, 1 mM $ZnCl_2$ buffer at pH 8.0 at 25 °C. Reversibility of the chemical denaturation was evaluated by subjecting the enzyme to decreasing urea dilutions from 8 M to 0.4 M.

2.10. Differential scanning calorimetry (DSC)

Transition temperatures (T_m) and enthalpies (ΔH_{cal}) were measured at 46 μM of *r*LAP using a nano-DSC system from TA

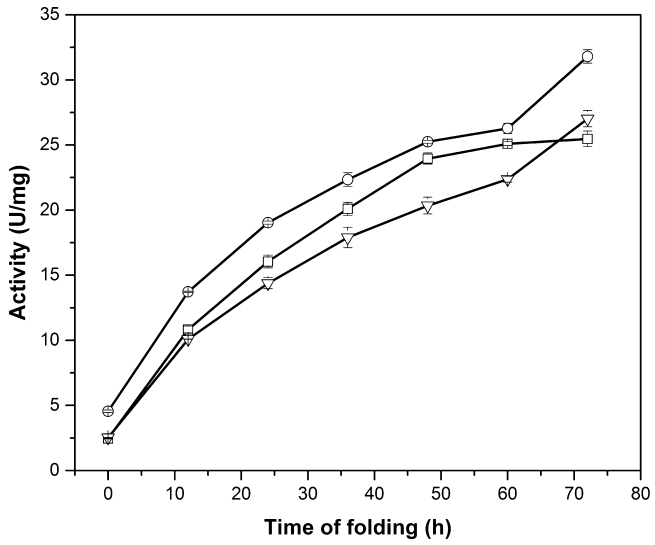

Fig. 1. Enzymatic activity of three in house-produced batches (LO11005 squares; LO12001 circles, and LO10004 triangles) of *r*LAP over the time of folding, under main folding conditions.

Instruments (New Castle, DE) equipped with a 300 μL platinum cell. Each sample was evaluated in triplicate at a scanning rate of 1 °C min^{-1}.

2.11. Free thiol analysis

Free thiols were derivatized using DyLight 488 Maleimide to a final concentration of 12.5 μM in a buffer of 100 mM phosphate at pH 8.0 [27]. The analysis was carried out in an ACQUITY UPLC System from Waters (Milford, MA), using a SEC column BEH 200, 4.1 × 300 mm, using a flow rate of 1.7 μM at a 0.4 mL min^{-1} for protein-fluorophore separation and quantification [28].

2.12. Mass spectrometry (MS)

Liquid chromatography electrospray ionization mass spectrometry (LC–ESI-MS, hereafter referred as MS) was performed in an ACQUITY UPLC System coupled to a SYNAPT G2 HDMS mass spectrometer from Waters (Milford, MA). A BEH300 C18 (1.7 μm) reverse phase column, UV detection at 214 nm, a flow rate of 0.3 mL min^{-1} at 70 °C and a linear gradient from 30 to 65% phase B (0.10% formic acid in acetonitrile) were used for LC analyses. Positive mode of ESI ionization source, 3.0 kV capillary voltage, 40 V cone voltage, 350 °C desolvation temperature, 120 °C source temperature, and acquisition range from 300 to 3500 *m*/*z* were used for MS analyses. MS data was analyzed using MaxEnt1 algorithm. The molecular masses of *r*LAP isoforms were calculated based on the amino acid sequence of the mature form of LAP$_{wt}$ [29].

3. Results

3.1. Functional and structural properties of rLAP

In a previous study we reported an increase in the enzymatic activity from 1 to 18 U/mg when 3 μM *r*LAP were incubated at 37 °C for 72 h in a buffer of 10 mM phosphate, 10 μM $ZnCl_2$ at pH 8.0 [22]. In this study we conducted exploratory tests by employing different pH values and buffers to assess the folding process of *r*LAP through its activity toward the optimization of the process. When tricine buffer at pH 8.0, or citrate buffer at pH 4.0, 5.0 or 6.0 were employed, the enzymatic activity remained below 2.5 U/mg. A subtle increase to 3 U/mg was observed using carbonate buffer at pH 8.5 and 9.0; however, when the pH increased to 10.0 the activity was totally lost after 72 h at 37 °C. An increase to 15 U/mg was observed after 72 h of incubation in phosphate buffer at pH 7.0 and 8.0, which remained similar to our original assessment, performed using a different batch of *r*LAP$_{uf}$ [22], however, when pH decreased down to 6.0, the specific activity of *r*LAP augmented to 31 U/mg after 72 h of incubation. The enzymatic activity of *r*LAP folded in phosphate buffer at pH 6.0, along with the aforementioned results at pH 8.0, suggests that the folding process was reproducible among batches (Fig. 1).

CD spectra revealed structural changes among: *r*LAP$_{fd}$, *r*LAP$_{uf}$, and LAP$_{wt}$ (Fig. 2). Although, the minimum negative ellipticity ($[\theta]_{mre}$) of these enzymes was centered at 208 nm (Fig. 2A), the CD spectrum intensity of *r*LAP$_{fd}$ was 0.4 times higher than the intensity of *r*LAP$_{uf}$, and 0.4 times lower compared to the intensity of LAP$_{wt}$.

IF spectrum of *r*LAP$_{fd}$ confirmed structural changes during the folding process, showing a decrease in the intensity of IF, and a blue shift of the λ_{max} from 330 to 325 nm exhibiting a closer profile to LAP$_{wt}$ (Fig. 2B). On the other hand, when *r*LAP$_{fd}$ was chemically denatured with urea revealed a red shift of its λ_{max} to 345 nm (Fig. 2B) and an increment in the intensity of its IF exhibiting a closer profile to *r*LAP$_{uf}$.

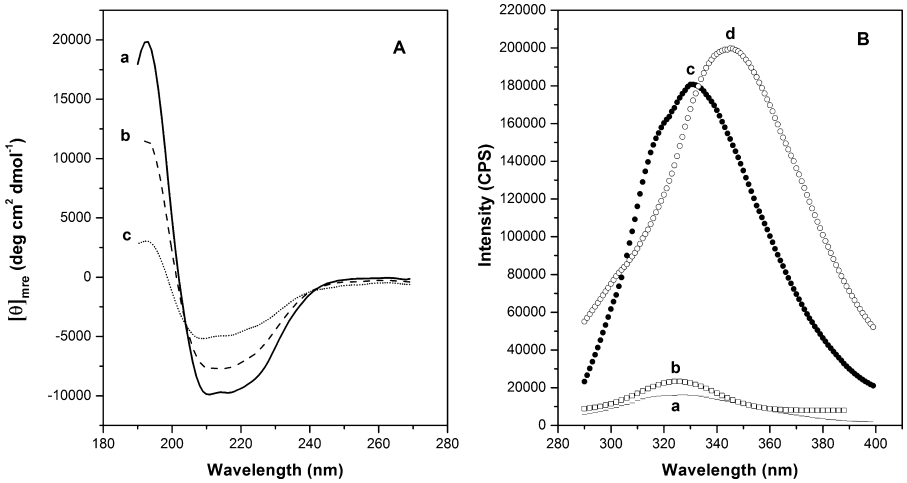

Fig. 2. (A) Circular dichroism spectra: LAP$_{wt}$ (A-a), *r*LAP$_{fd}$ (A-b), and *r*LAP$_{uf}$ (A-c). (B) Intrinsic fluorescence spectra: LAP$_{wt}$ (B-a), *r*LAP$_{fd}$ (B-b), *r*LAP$_{uf}$ (B-c), and *r*LAP$_{uf}$ denatured in 8 M urea (B-d).

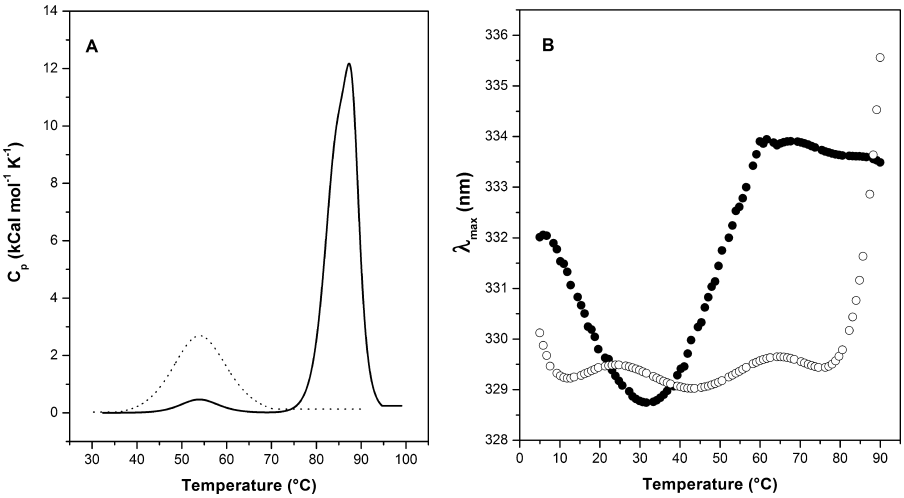

Fig. 3. (A) Thermal unfolding of *r*LAP analyzed by DSC; *r*LAP$_{uf}$ (short-dot line) exhibits only one T_m at 54 °C, where as *r*LAP$_{fd}$ (solid line) exhibits three T_m at 54, 85, and 88 °C. (B) Thermal denaturation of *r*LAP analyzed by IF; *r*LAP$_{uf}$ (closed circles) exhibits two inflection points (16 °C and 50 °C), whereas *r*LAP$_{fd}$ exhibited only one around 85 °C.

Table 1
Thermodynamic parameters of *r*LAP by DSC.

Sample	T_{m_1} (°C)	T_{m_2} (°C)	T_{m_3} (°C)	ΔH_1 (kCal mol^{-1})	ΔH_2 (kCal mol^{-1})	ΔH_3 (kCal mol^{-1})	ΔH_{cal} (kCal mol^{-1})
*r*LAP$_{uf}$	54 ± 0.1	NP	NP	55 ± 2	NP	NP	55 ± 2
*r*LAP$_{fd}$	54 ± 0.3	85 ± 0.4	88 ± 0.1	4 ± 1	65 ± 3	31 ± 2	100 ± 5

NP: not present.

3.2. Thermal stability of rLAP

Thermal stability evaluated through DSC showed that *r*LAP$_{fd}$ exhibited three different T_m (54, 85, and 88 °C) while *r*LAP$_{uf}$ only exhibited one T_m at 54 °C (Fig. 3A and Table 1). The transition at 54 °C found in both, folded and unfolded enzyme, exhibited enthalpies that differed in about 13 times, where the higher enthalpy was observed in *r*LAP$_{uf}$ (Table 1). The total enthalpy (ΔH_{cal}) differed in almost two times between *r*LAP$_{fd}$ and *r*LAP$_{uf}$.

Thermal denaturation of *r*LAP was analyzed by IF, and showed a different behavior between *r*LAP$_{uf}$ and *r*LAP$_{fd}$ (Fig. 3B). For *r*LAP$_{uf}$, λ_{max} behavior was defined by temperature regions, where the displacement below 35 °C shifted toward blue fluorescence, whereas above this temperature shifted toward red fluorescence. In addition, when λ_{max} of *r*LAP$_{uf}$ was analyzed as the first derivative in function of the temperature ($d\lambda_{max}/dt$) a minimum and a maximum inflection points (at 16 °C and 50 °C, respectively) were observed. A thermal transition was observed around 85 °C for *r*LAP$_{fd}$.

3.3. Urea-induced unfolding of rLAP by lifetime and intrinsic fluorescence

The values of τ and λ_{max} (Fig. 4) augmented as the concentration of urea increased, although τ showed a marked inflection across the denaturation gradient in both, folded or unfolded enzymes. Fluorescence lifetime values and χ^2 (as the measure of fitting) of *r*LAP and LAP$_{wt}$ are shown in Table 2. Another interesting result is that the τ value of *r*LAP$_{fd}$ is the closest to the τ value of LAP$_{wt}$.

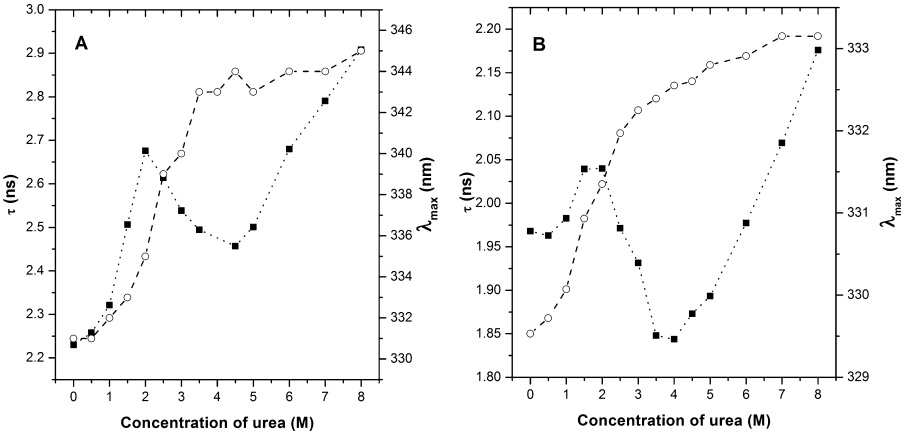

Fig. 4. Chemical denaturation of *r*LAP in function of the urea concentration assessed by τ (solid squares) and λ_{max} (open circles). (A) The range of τ between the initial and the final stress levels for *r*LAP$_{uf}$ was 2.20–2.90 ns, with a red shift of λ_{max} from 331 to 345 nm. (B) The range of τ for *r*LAP$_{fd}$ was from 1.97 to 2.15 ns and its λ_{max} was from 330 nm to 333 nm.

Table 2
Fluorescence lifetime values of *r*LAP.

Protein	τ (ns)	χ^2
LAP_{wt}	1.61	1.20
$rLAP_{uf}$	2.23	1.20
$rLAP_{uf}$ in 8 M urea	2.91	1.26
$rLAP_{fd}$	1.96	1.16
$rLAP_{fd}$ in 8 M urea	2.17	1.24

Data fitted using two exponential decays.

3.4. Reversibility of the urea-induced unfolding process

The enzymatic activity evaluated at several dilutions of urea, from 8 M to 0.4 M, at 25 °C, showed that the enzymatic activity increased as the urea concentration was diluted (Fig. 5).

3.5. Folding promoted the formation of disulfide bond of rLAP

A 0.54 mol of free cysteines/mol of protein ratio was observed for $rLAP_{uf}$, whereas for $rLAP_{fd}$ the ratio was 0.34 mol of cysteines/mol of protein. In regard to an implicit amount of *r*LAP molecules that buried free cysteines as disulfide bonds (S—S) (without any consideration of thiol oxidation, improper S—S bonding, or other degradation), an increase from 47% (for $rLAP_{uf}$) to 66% (for $rLAP_{fd}$) was observed (Fig. 6).

3.6. Mass spectrometry analysis

Due to the increase in the enzymatic activity after folding, we considered the possibility that the enzyme was capable to self-catalyze its 6×-His tag as suggested by other researchers [18]. To explore this hypothesis we evaluated the enzyme by mass spectrometry during 15 days of incubation at 15 °C. As shown in Fig. 7A and B, the enzyme exhibits the same distribution of mass isoforms at the beginning and at the end of the folding process (Fig. 7C); the mass of each isoform is summarized in Table 3.

The enzyme activity was also determined during this incubation period (Fig. 7D); an increase in the activity was observed from 2.1 ± 0.1, and 8.5 ± 0.1 U/mg, at the beginning and the end of the folding period respectively.

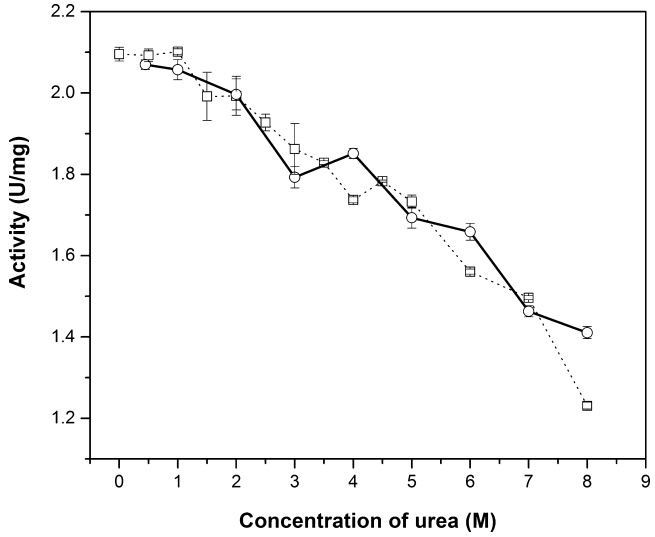

Fig. 5. Evaluation of the reversibility of the urea-induced denaturation of *r*LAP. The open squares curve shows the denaturation process of the enzyme as the concentration of urea was increased, while the open circles curve shows the reversibility of the denaturation process as the urea concentration was diluted.

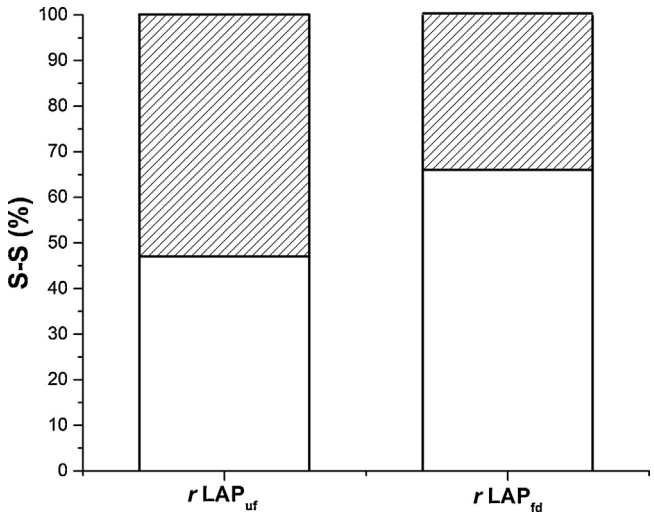

Fig. 6. Percentage of established (white area) and non-established disulfide bonds (shaded area) for $rLAP_{uf}$ and $rLAP_{fd}$.

3.7. Effect of enzyme and zinc concentration on folding through the activity of rLAP

To evaluate the feasibility of scaling up the folding process, different concentrations of *r*LAP and $ZnCl_2$ were tested from an enzymatic activity perspective: (1) 30 μM and 20 μM, (2) 152 μM and 50 μM, and (3) 305 μM and 100 μM, respectively. No more than 7 U/mg of enzymatic activity was observed when the concentration of enzyme and $ZnCl_2$ were augmented (Fig. 8).

4. Discussion

4.1. Structure and activity of rLAP after folding

The biological activity of a protein is strongly linked to its conformation; thus, is expected that structural changes may have a positive or negative impact on its functionality [10,20,30,31]. It have been reported that N-and C-terminal propeptides are essential for the folding of *r*LAP when it was expressed in *E. coli* [32,33]; however, we were capable of expressing a mature protein fused to the 6×-His tag in N-terminal, and determine the optimal folding conditions by testing different buffer solutions and pH values, where the higher activity was 31 U/mg when the protein was incubated in phosphate buffer at pH 6.0 (Fig. 1).

The increase of the enzymatic activity at pH 6.0 is potentially associated to the couple of two zinc atoms with the two histidines along with other residues (mainly acidic) located in the catalytic site through coordinate covalent bonds. At pH 6.0 the theoretical relative amount of cationic zinc species is about 90% (as denoted by the ion distribution as function of pH in the zinc-gluconic acid system) [34], whereas the deprotonated imidazole groups of the histidines (which have a pK_a of 6.02) would be around 50%, resulting

Table 3
Isoforms molecular masses of *r*LAP obtained by LC–ESI-MS.

Symbol	Isoforms of *r*LAP	Molecular mass (Da)
A	Met – 6 His tag – *r*LAP	32,828
B	6 His tag – *r*LAP	32,665
C	5 His tag – *r*LAP	32,528
D	4 His tag – *r*LAP	32,391
E	3 His tag – *r*LAP	32,253
F	2 His tag – *r*LAP	32,116
G	1 His tag – *r*LAP	31,995
H	*r*LAP	31,880

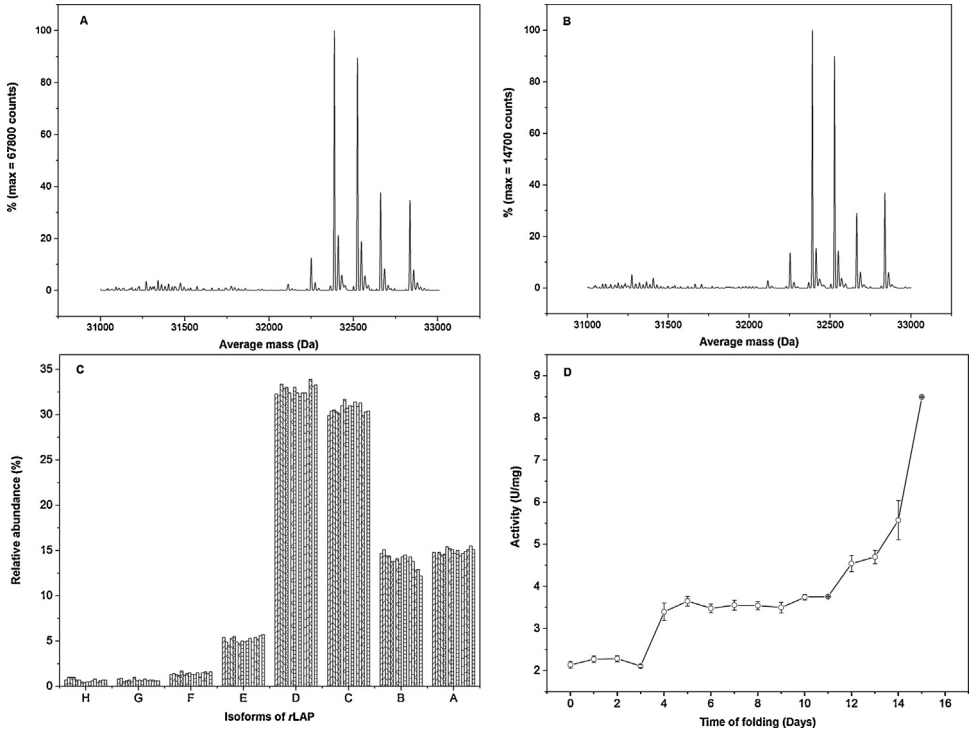

Fig. 7. Spectrograms obtained from the MS analyses of *r*LAP. Deconvoluted mass spectra at: (A) 0, and (B) 15 days of incubation; (C) relative abundance of *r*LAP isoforms, each group of bars contains 0–15 days of incubation from left to right; and (D) enzyme activity monitored throughout the whole folding period.

favorable for their binding [35]. This electrostatic interaction also explains the absence of enzymatic activity when the citrate buffer system is used for folding, even at pH 4.0, because cationic species of zinc (above the 50% of relative abundance) are theoretically only present at pH lower than 3.7 under the Zn-citric acid system [36], which is no longer useful, due to the imidazole substituent pK_a.

Under the phosphate buffer conditions, the zinc speciation behavior should be more similar to the observed in the gluconic acid system rather than in the citric acid system, based on the phosphate

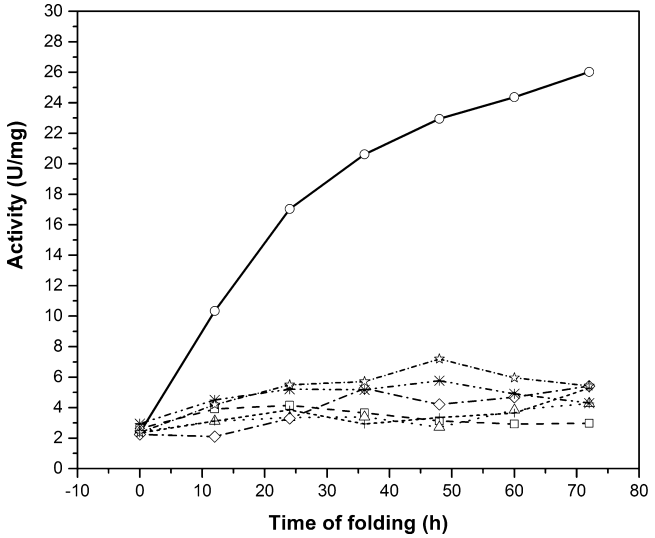

Fig. 8. Curves of enzymatic activity of *r*LAP under different folding conditions: (1) circles represent 3 μM *r*LAP, and 10 μM $ZnCl_2$; (2) squares 30 μM *r*LAP, and 10 μM $ZnCl_2$; (3) triangles 152 μM *r*LAP, and 10 μM $ZnCl_2$; (4) diamonds 305 μM *r*LAP, and 10 μM $ZnCl_2$; (5) asterisks 30 μM *r*LAP, and 20 μM $ZnCl_2$; (6) stars 152 μM *r*LAP, and 50 μM $ZnCl_2$; and (7) cross 305 μM *r*LAP, and 100 μM $ZnCl_2$.

second pK_a around 6.0. This also could explain the reason why the enzymatic activity remains similar to the activity of the unfolded protein at pH below or above 6.0, despite that the enzyme was subjected to folding (see results in Section 3.1).

The increase in the activity of *r*LAP was attributable to structural changes, which was confirmed by the comparison of the conformation of $rLAP_{uf}$, $rLAP_{fd}$ and the LAP_{wt}, through spectroscopic techniques (Fig. 2). The dichroic response indicated that there was a gaining in structure in $rLAP_{fd}$ with respect to $rLAP_{uf}$. The decrease in intensity, and the blue shift of the λ_{max} observed by IF in $rLAP_{fd}$, was an indicator of the most folded conformation of the enzyme as well (Fig. 2B), as have been observed in proteins that contain buried tryptophans [11,37,38].

Disulfide bonds also play a key role in promoting and maintaining a more stable conformation of proteins [4,39], due to an increase in their thermal stability. Is well known that LAP_{wt} has a unique disulfide bond that relies on the hydrophobic pocket adjacent to the active site [23]; in our study the number of established bonds was indirectly estimated by the quantification of free cysteines. The results showed that the increase of the enzymatic activity could be associated to an additional 20% in the formation of disulfide bonds in $rLAP_{fd}$ (Fig. 6) and consequently to a gaining in structure for the active site. On the other hand, when the protein was not folding-processed, the level of free cysteines was higher than in the folding-processed protein; which is an indicator of a lower level of established disulfide bonds in $rLAP_{uf}$, which stands for a less structured protein.

The slow progression of *r*LAP folding (Fig. 1) might be related to the cis/trans isomerization of the peptide bond [40–42], which in other proteins takes to the appropriate formation of the disulfide bond [40], that in *r*LAP are adjacent to the catalytic site. The cis-peptide bond in LAP_{wt} is located between the Asp-117 and the Asp-118 in its folded conformation [23], although *r*LAP came through different expression and purification conditions than LAP_{wt}, it also contains this particular sequence, thus it is possible

that its folding takes longer due to the slow establishment of a correct cis/trans configuration followed by the establishment of the disulfide bond; as have been reported for cytrochrome *c* whose fast or slow folding are determined by already present specific motifs in its molten globule state [12].

The results obtained so far helped us to understand the factors that impact on the folding process, and consequently to improve the downstream process toward a more stable and functional enzyme for industrial purposes. On this regard, the effect of the enzyme and $ZnCl_2$ concentrations during folding evaluated through the enzymatic activity showed that the increase in the concentration of the enzyme reduces the folding yield, even if we increased $ZnCl_2$ concentration (Fig. 8).

4.2. Increased thermal stability of rLAP

It is well known that thermal stability of a protein is related to its level of covalent and non-covalent bonds that maintain an organized structure [43–45]. Herein, we observed a positive effect of folding in the thermodynamic stability of *r*LAP that increased its T_m, (Fig. 3, and Table 1) which is an indicator of a higher number of hydrogen bonds and disulfide bonds, also consistent with the free cysteines analysis (Fig. 6). The results obtained by DSC suggest that the T_m found at 54 °C in $rLAP_{fd}$ corresponds to a residual amount of $rLAP_{uf}$, whereas the transitions at 85 and 88 °C in $rLAP_{fd}$ correspond to a more folded protein that increases its ration after folding (Fig. 3A, and Table 1). In addition, IF confirms a higher stability of $rLAP_{fd}$ up to 85 °C when a red displacement of λ_{max} was observed (Fig. 3B) which is consistent with previous IF responses in other protein studies [46–48]. For $rLAP_{uf}$ IF revealed that the folding process occurs below 40 °C, based on the blue shift of λ_{max}, whereas the thermal denaturation takes place from 40 °C until 60° C. Unlike to IF, DSC has a lower sensitivity to detect gradual molecular transitions of subtle exothermic enthalpies during the establishment of hydrogen bonds; however, it is capable to detect the single endothermic transition that comprises the rupture of all the non-covalent interactions.

4.3. Chemical stability of rLAP

Urea was employed as chaotropic agent to denature $rLAP_{uf}$ and $rLAP_{fd}$ to compare their chemical stability at different stress levels (0–8 Murea) (Fig. 4); $rLAP_{uf}$ exhibited a wider range of τ between the initial and the final levels of the denaturation curve (2.23–2.90 ns), with respect to $rLAP_{fd}$ (τ from 1.97 to 2.17 ns). On the other hand, the red displacement of λ_{max} after denaturation is higher in $rLAP_{uf}$ (331–345 nm) than in $rLAP_{fd}$ (330–333 nm), which was chemically more stable.

As part of the extended characterization of *r*LAP, we observed that urea-induced denaturation of $rLAP_{uf}$ was a reversible process, since the protein recovered its enzymatic activity as the urea was diluted (Fig. 5). These results demonstrated that once *r*LAP is produced as insoluble inclusion bodies in *E. coli*, it would be feasible to increase its enzymatic activity through folding, even after stressful solubilization procedures that are typically employed for harvesting the protein from insoluble inclusion bodies.

4.4. Molecular mass distribution of rLAP during folding

The relative abundance of all the molecular masses isoforms of *r*LAP was maintained across the folding process (Fig. 7C, and Table 3). There was no evidence that the enzyme was capable of self-catalyze; hence, the increase in the enzymatic activity (Fig. 7D) is more likely to be associated to structural changes as have been discussed throughout this study.

5. Conclusion

The collective information obtained from the spectroscopic and thermodynamic techniques, along with the enzymatic assays employed on this study, are valuable for describing the folding processing of *r*LAP, and the way that pH favored the coupling of zinc to the catalytic site. These findings allowed the establishment of a characterization approach for a better understanding of the folding process in bimetallic proteins. Hence, the conditions of folding for *r*LAP were optimized with respect to our previous study, since we obtained a recombinant enzyme with a higher activity resulting from a better structural stability associated to the folding treatment. In this sense, orthogonal techniques represent an advantageous approach for distinguishing phenomena that occur at different molecular levels during the folding process of a protein that could be helpful for a better understanding of the processes toward their improvement.

Acknowledgements

The authors thank to Antonio Hernández-García, Maribel Jardón-Castillo, and Mario E. Abad-Javier, for their technical contribution in the cysteines quantification, fluorescence, and calorimetric techniques at the Research and Development Unit of PROBIOMED S.A. de C.V.

References

[1] T. Dingermann, Biotechnol. J. 3 (2008) 90–97.
[2] K. Graumann, A. Premstaller, Biotechnol. J. 1 (2006) 164–186.
[3] A. Villaverde, M. Mar Carrió, Biotechnol. Lett. 25 (2003) 1385–1395.
[4] R. Rudolph, H. Lilie, FASEB J. 10 (1996) 49–56.
[5] E. De Bernardez Clark, Curr. Opin. Biotechnol. 9 (1998) 157–163.
[6] L. Grillberger, T.R. Kreil, S. Nasr, M. Reiter, Biotechnol. J. 4 (2009) 186–201.
[7] E.M. Gorman, B.E. Padden, E.J. Munson, S.C. Gad, Stability: physical and chemical, in: Pharmaceutical Sciences Encyclopedia, John Wiley & Sons, Inc., 2010.
[8] C. Tanford, M.L. Anson, J.T. Edsall, C.B. Anfinsen, M.R. Frederic, Protein denaturation, in: Advances in Protein Chemistry, Academic Press, 1968, pp. 121–282.
[9] K. Hejnaes, F. Matthiesen, L. Skriver, Protein stability in downstream processing, in: Bioseparation and Bioprocessing, Wiley-VCH Verlag GmbH, 2008, pp. 31–65.
[10] A. Fersht, Structure and Mechanism in Protein Science, 2nd ed., W. H. Freeman and Company, New York, 1999.
[11] J.R. Lakowicz, Fluorescence sensing, in: Principles of Fluorescence Spectroscopy, Springer US, 2006, pp. 623–673.
[12] T.R. Sosnick, L. Mayne, R. Hiller, S.W. Englander, Struct. Biol. 1 (1994) 149–156.
[13] K.A. Dill, J.L. MacCallum, Science 338 (2012) 1042–1046.
[14] A.G. Szabo, D.M. Rayner, J. Am. Chem. Soc. 102 (1980) 554–563.
[15] M.Y. Berezin, S. Achilefu, Chem. Rev. 110 (2010) 2641–2684.
[16] J.R. Lakowicz, M.R. Eftink, Intrinsic fluorescence of proteins, in: Topics in Fluorescence Spectroscopy, Springer US, 2002, pp. 1–15.
[17] G. Pérez-Sánchez, L.I. Leal-Guadarrama, I. Trelles, N.O. Pérez, E. Medina-Rivero, Process Biochem. 46 (2011) 1825–1830.
[18] M. Hartley, B. Bennett, Protein Expr. Purif. 66 (2009) 91–101.
[19] R.C. Holz, Coord. Chem. Rev. 232 (2001) 5–26.
[20] A. Taylor, J. Fed. Am. Soc. Exp. Biol. 7 (1993) 290–298.
[21] M. Matsui, J.H. Fowler, L.L. Walling, Biol. Chem. 387 (2006) 1535–1544.
[22] A.V. Hernández-Moreno, F. Villaseñor, E. Medina-Rivero, N.O. Pérez, L.F. Flores-Ortiz, G. Saab-Rincón, G. Luna-Bárcenas, Int. J. Biol. Macromol. 64 (2014) 306–312.
[23] B. Chevrier, C. Schalk, H. D'Orchymont, J.-M. Rondeau, D. Moras, C. Tarnus, Structure 2 (1994) 283–291.
[24] K.P. Bzymek, S.I. Swierczek, B. Bennett, R.C. Holz, Inorg. Chem. 44 (2005) 8574–8580.
[25] J.R. Lakowicz, Time-domain lifetime measurements, in: Principles of Fluorescence Spectroscopy, Springer US, 2006, pp. 97–155.
[26] V. Kayser, N. Chennamsetty, V. Voynov, B. Helk, B. Trout, J. Fluoresc. 21 (2011) 275–288.
[27] C. Zhang, C. Rodriguez, M. Circu, T. Aw, J. Feng, Anal. Bioanal. Chem. 401 (2011) 2165–2175.
[28] G.T. Hermanson, Bioconjugate Techniques, 2nd ed., 2008, San Diego, CA, USA.
[29] C. Guenet, P. Lepage, B.A. Harris, J. Biol. Chem. 267 (1992) 8390–8395.
[30] T.E. Creighton, Proteins. Structures and Molecular Properties, 2nd ed., W. H. Freeman and Company, New York, 1993.
[31] J.R. Lakowicz, S. D' Auria, M. Rossi, I. Gryczynski, Fluorescence of Extreme thermophilic proteins, in: Topics in Fluorescence Spectroscopy, Springer US, 2002, pp. 285–306.

[32] Z.-Z. Zhang, S. Nirasawa, Y. Nakajima, M. Yoshida, K. Hayashi, Biochemistry 350 (2000) 671–676.
[33] S. Nirasawa, Y. Nakajima, Z.-Z. Zhang, M. Yoshida, K. Hayashi, Biochemistry 341 (1999) 25–31.
[34] M. Dekker, Handbook of Metal–Ligand Interaction in Bilogic Fluids – Bioinorganic Medicine, 1995, New York.
[35] L. Zhou, S. Li, Y. Su, X. Yi, A. Zheng, F. Deng, J. Phys. Chem. B 117 (2013) 8954–8965.
[36] R.B. Martin, Antimicrob. Agents Chemother. 32 (1988) 608–609.
[37] M.R. Eftink, C.A. Ghiron, Biochemistry 15 (1976) 672–680.
[38] J.T. Vivian, P.R. Callis, Biophys. J. 80 (2001) 2093–2109.
[39] C. Tanford, J.T. Edsall, C.B. Anfinsen, M.R. Frederic, Protein denaturation. Part C: Theoretical models for the mechanism of denaturation, in: Advances in Protein Chemistry, Academic Press, 1970, pp. 1–95.
[40] F.X. Schmid, Ann. Rev. Biophys. Bimol. Struct. 22 (1993) 123–143.
[41] W.J. Wedemeyer, E. Welker, H.A. Scheraga, Biochemistry 41 (2002) 14637–14644.
[42] K. Lang, F.X. Schmid, G. Fischer, Nature 329 (1987) 268–270.
[43] P.L. Privalov, Stability of proteins, in: Advances in Protein Chemistry, Academic Press, 1982, pp. 1–104.
[44] G. Privalov, V. Kavina, E. Freire, P.L. Privalov, Anal. Biochem. 232 (1995) 79–85.
[45] S.P. Manly, K.S. Matthews, J.M. Sturtevant, Biochemistry 24 (1885) 3842–3846.
[46] A.I. Dragan, P.L. Privalov, J. Mol. Biol. 321 (2002) 891–908.
[47] T.Q. Faria, J.C. Lima, M. Bastos, A.L. Maçanita, H. Santos, J. Biol. Chem. 279 (2004) 48680–48691.
[48] M. Weichel, S. Bassarab, P. Garidel, Bioprocess Tech. 6 (2008) 42–45.